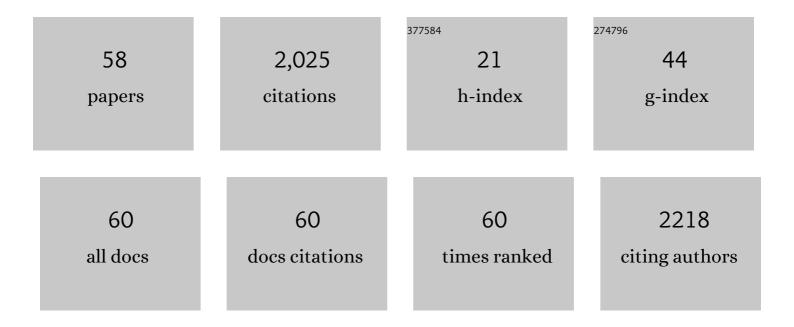
Jennifer M Renaud

List of Publications by Year in descending order

Source: https://exaly.com/author-pdf/5462642/publications.pdf Version: 2024-02-01



#	Article	lF	CITATIONS
1	Myocardial flow reserve estimation with contemporary CZT-SPECT and 99mTc-tracers lacks precision for routine clinical application. Journal of Nuclear Cardiology, 2022, 29, 2078-2089.	1.4	12
2	Effect of iterations and time of flight on normal distributions of 82Rb PET relative perfusion and myocardial blood flow. Journal of Nuclear Cardiology, 2022, 29, 2612-2623.	1.4	3
3	Does quantification of [11C]meta-hydroxyephedrine and [13N]ammonia kinetics improve risk stratification in ischemic cardiomyopathy. Journal of Nuclear Cardiology, 2022, 29, 413-425.	1.4	1
4	Impact of residual subtraction on myocardial blood flow and reserve estimates from rapid dynamic PET protocols. Journal of Nuclear Cardiology, 2022, 29, 2262-2270.	1.4	3
5	Evaluation of Lung Glucose Uptake with Fluorine-18 Fluorodeoxyglucose Positron Emission Tomography/CT in Patients with Pulmonary Arterial Hypertension and Pulmonary Hypertension Due to Left Heart Disease. Annals of Nuclear Cardiology, 2022, , .	0.0	0
6	Increased myocardial oxygen consumption rates are associated with maladaptive right ventricular remodeling and decreased event-free survival in heart failure patients. Journal of Nuclear Cardiology, 2021, 28, 2784-2795.	1.4	8
7	Site qualification and clinical interpretation standards for 99mTc-SPECT perfusion imaging in a multi-center study of MITNEC (Medical Imaging Trials Network of Canada). Journal of Nuclear Cardiology, 2021, 28, 2712-2725.	1.4	1
8	Reproducible Quantification of Regional Sympathetic Denervation with [11C]meta-Hydroxyephedrine PET Imaging. Journal of Nuclear Cardiology, 2021, 28, 2745-2757.	1.4	5
9	Patient-specific SPECT imaging protocols to standardize image noise. Journal of Nuclear Cardiology, 2021, 28, 225-233.	1.4	3
10	Quantitative clinical nuclear cardiology, part 2: Evolving/emerging applications. Journal of Nuclear Cardiology, 2021, 28, 115-127.	1.4	15
11	Quantitative clinical nuclear cardiology, part 2: Evolving/emerging applications. Journal of Nuclear Medicine, 2021, 62, 168-176.	2.8	5
12	Internal validation of myocardial flow reserve PET imaging using stress/rest myocardial activity ratios with Rb-82 and N-13-ammonia. Journal of Nuclear Cardiology, 2021, 28, 835-850.	1.4	6
13	Effects of two patient-specific dosing protocols on measurement of myocardial blood flow with 3D 82Rb cardiac PET. European Journal of Nuclear Medicine and Molecular Imaging, 2021, 48, 3835-3846.	3.3	5
14	Reliable quantification of myocardial sympathetic innervation and regional denervation using [11C]meta-hydroxyephedrine PET. European Journal of Nuclear Medicine and Molecular Imaging, 2020, 47, 1722-1735.	3.3	7
15	Letter to the editor: Lassen et al. 3D PET/CT 82Rb PET myocardial blood flow quantification: comparison of half-dose and full-dose protocols. European Journal of Nuclear Medicine and Molecular Imaging, 2020, 47, 2729-2730.	3.3	1
16	Application of Hybrid Matrix Metalloproteinase-Targeted and Dynamic ²⁰¹ Tl Single-Photon Emission Computed Tomography/Computed Tomography Imaging for Evaluation of Early Post-Myocardial Infarction Remodeling. Circulation: Cardiovascular Imaging, 2019, 12, e009055.	1.3	18
17	Angiotensin Receptor Neprilysin Inhibitor Attenuates Myocardial Remodeling and Improves Infarct Perfusion in Experimental Heart Failure. Scientific Reports, 2019, 9, 5791.	1.6	43
18	[¹⁸ F]FDG cardiac PET imaging in a canine model of radiation-induced cardiovascular disease associated with breast cancer radiotherapy. American Journal of Physiology - Heart and Circulatory Physiology, 2019, 316, H586-H595.	1.5	12

Jennifer M Renaud

#	Article	IF	CITATIONS
19	Saline-push improves rubidium-82 PET image quality. Journal of Nuclear Cardiology, 2019, 26, 1869-1874.	1.4	7
20	Repeatable and reproducible measurements of myocardial oxidative metabolism, blood flow and external efficiency using 11C-acetate PET. Journal of Nuclear Cardiology, 2018, 25, 1912-1925.	1.4	13
21	Consistent tracer administration profile improves test–retest repeatability of myocardial blood flow quantification with 82Rb dynamic PET imaging. Journal of Nuclear Cardiology, 2018, 25, 929-941.	1.4	45
22	Reproducible quantification of cardiac sympathetic innervation using graphical modeling of carbon-11-meta-hydroxyephedrine kinetics with dynamic PET-CT imaging. EJNMMI Research, 2018, 8, 63.	1.1	9
23	Effects of Riociguat on Right Ventricular Remodelling in Chronic Thromboembolic Pulmonary Hypertension Patients: A Prospective Study. Canadian Journal of Cardiology, 2018, 34, 1137-1144.	0.8	9
24	Inter- and Intraobserver Agreement of ¹⁸ F-FDG PET/CT Image Interpretation in Patients Referred for Assessment of Cardiac Sarcoidosis. Journal of Nuclear Medicine, 2017, 58, 1324-1329.	2.8	32
25	Optimization of SPECT Measurement of Myocardial Blood Flow with Corrections for Attenuation, Motion, and Blood Binding Compared with PET. Journal of Nuclear Medicine, 2017, 58, 2013-2019.	2.8	88
26	Characterization of 3-Dimensional PET Systems for Accurate Quantification of Myocardial Blood Flow. Journal of Nuclear Medicine, 2017, 58, 103-109.	2.8	61
27	Optimally Repeatable Kinetic Model Variant for Myocardial Blood Flow Measurements with ⁸² Rb PET. Computational and Mathematical Methods in Medicine, 2017, 2017, 1-11.	0.7	8
28	Dual Spillover Correction for SPECT Myocardial Blood Flow Measurement. , 2017, , .		0
29	Reply: Variation in Maximum Counting Rates During Myocardial Blood Flow Quantification Using ⁸² Rb PET. Journal of Nuclear Medicine, 2017, 58, 519-520.	2.8	3
30	Comparison of 18F-fluorodeoxyglucose positron emission tomography (FDG PET) and cardiac magnetic resonance (CMR) in corticosteroid-naive patients with conduction system disease due to cardiac sarcoidosis. European Journal of Nuclear Medicine and Molecular Imaging, 2016, 43, 259-269.	3.3	73
31	PET Metabolic Biomarkers for Cancer. Biomarkers in Cancer, 2016, 8s2, BIC.S27483.	3.6	17
32	Radionuclide Tracers for Myocardial Perfusion Imaging and Blood Flow Quantification. Cardiology Clinics, 2016, 34, 37-46.	0.9	15
33	Myocardial blood flow quantification by Rb-82 cardiac PET/CT: A detailed reproducibility study between two semi-automatic analysis programs. Journal of Nuclear Cardiology, 2016, 23, 499-510.	1.4	29
34	Shifts in myocardial fatty acid and glucose metabolism in pulmonary arterial hypertension: a potential mechanism for a maladaptive right ventricular response. European Heart Journal Cardiovascular Imaging, 2016, 17, 1424-1431.	0.5	53
35	Single low-dose CT scan optimized for rest-stress PET attenuation correction and quantification of coronary artery calcium. Journal of Nuclear Cardiology, 2015, 22, 419-428.	1.4	27
36	Test–retest repeatability of myocardial blood flow and infarct size using 11C-acetate micro-PET imaging in mice. European Journal of Nuclear Medicine and Molecular Imaging, 2015, 42, 1589-1600.	3.3	8

Jennifer M Renaud

#	Article	IF	CITATIONS
37	l ² 2-adrenergic stress evaluation of coronary endothelial-dependent vasodilator function in mice using 11C-acetate micro-PET imaging of myocardial blood flow and oxidative metabolism. EJNMMI Research, 2014, 4, 68.	1.1	6
38	Effects of Short-Term Continuous Positive Airway Pressure on Myocardial Sympathetic Nerve Function and Energetics in Patients With Heart Failure and Obstructive Sleep Apnea. Circulation, 2014, 130, 892-901.	1.6	80
39	Clinical Interpretation Standards and Quality Assurance for the Multicenter PET/CT Trial Rubidium-ARMI. Journal of Nuclear Medicine, 2014, 55, 58-64.	2.8	40
40	The role of integrin α2 in cell and matrix therapy that improves perfusion, viability and function of infarcted myocardium. Biomaterials, 2014, 35, 4749-4758.	5.7	34
41	Cardiac Micro-PET-CT. Current Cardiovascular Imaging Reports, 2013, 6, 179-190.	0.4	0
42	Characterizing the normal range of myocardial blood flow with 82rubidium and 13N-ammonia PET imaging. Journal of Nuclear Cardiology, 2013, 20, 578-591.	1.4	54
43	Test–retest repeatability of quantitative cardiac 11C-meta-hydroxyephedrine measurements in rats by small animal positron emission tomography. Nuclear Medicine and Biology, 2013, 40, 676-681.	0.3	28
44	Preclinical Evaluation of Biopolymer-Delivered Circulating Angiogenic Cells in a Swine Model of Hibernating Myocardium. Circulation: Cardiovascular Imaging, 2013, 6, 982-991.	1.3	10
45	Is There an Association Between Clinical Presentation and the Location and Extent of Myocardial Involvement of Cardiac Sarcoidosis as Assessed by ¹⁸ F- Fluorodoexyglucose Positron Emission Tomography?. Circulation: Cardiovascular Imaging, 2013, 6, 617-626.	1.3	83
46	Repeatable Noninvasive Measurement of Mouse Myocardial Glucose Uptake with ¹⁸ F-FDG: Evaluation of Tracer Kinetics in a Type 1 Diabetes Model. Journal of Nuclear Medicine, 2013, 54, 1637-1644.	2.8	35
47	PET Instrumentation. , 2013, , 127-137.		0
48	¹⁸ F-FDG Cell Labeling May Underestimate Transplanted Cell Homing: More Accurate, Efficient, and Stable Cell Labeling with Hexadecyl-4-[¹⁸ F]Fluorobenzoate for in Vivo Tracking of Transplanted Human Progenitor Cells by Positron Emission Tomography. Cell Transplantation, 2012, 21, 1821-1835.	1.2	29
49	Uniformity and repeatability of normal resting myocardial blood flow in rats using [13N]-ammonia and small animal PET. Nuclear Medicine Communications, 2012, 33, 917-925.	0.5	11
50	Accuracy of low-dose rubidium-82 myocardial perfusion imaging for detection of coronary artery disease using 3D PET and normal database interpretation. Journal of Nuclear Cardiology, 2012, 19, 1135-1145.	1.4	40
51	Does quantification of myocardial flow reserve using rubidium-82 positron emission tomography facilitate detection of multivessel coronary artery disease?. Journal of Nuclear Cardiology, 2012, 19, 670-680.	1.4	252
52	Impaired Myocardial Flow Reserve on Rubidium-82 Positron Emission Tomography Imaging Predicts Adverse Outcomes in Patients Assessed for Myocardial Ischemia. Journal of the American College of Cardiology, 2011, 58, 740-748.	1.2	498
53	Altered myocardial glucose utilization and the reverse mismatch pattern on rubidium-82 perfusion/F-18-FDG PET during the sub-acute phase following reperfusion of acute anterior myocardial infarction. Journal of Nuclear Cardiology, 2011, 18, 657-667.	1.4	16
54	PET of (<i>R</i>)- ¹¹ C-Rolipram Binding to Phosphodiesterase-4 Is Reproducible and Sensitive to Increased Norepinephrine in the Rat Heart. Journal of Nuclear Medicine, 2011, 52, 263-269.	2.8	16

#	Article	IF	CITATIONS
55	Intra- and inter-operator repeatability of myocardial blood flow and myocardial flow reserve measurements using rubidium-82 pet and a highly automated analysis program. Journal of Nuclear Cardiology, 2010, 17, 600-616.	1.4	126
56	In Vivo Assessment of Myocardial Glucose Uptake by Positron Emission Tomography in Adults With the <i>PRKAG2</i> Cardiac Syndrome. Circulation: Cardiovascular Imaging, 2009, 2, 485-491.	1.3	15
57	3D list-mode cardiac PET for simultaneous quantification of myocardial blood flow and ventricular function. , 2008, , .		6
58	Quantification of the normal range of myocardial blood flow and flow reserve with ⁸² rubidium versus ¹³ N-ammonia PET. , 2007, , .		0